NASA TECHNICAL NOTE

NASA TN D-5557

c.1

NASA TN D-5557

SOME FACTORS AFFECTING THE STRESS-CORROSION CRACKING OF Ti-6Al-4V ALLOY IN METHANOL

by W. Barry Lisagor

Langley Research Center
Langley Station, Hampton, Va.

1. Report No. NASA TN D-5557	2. Government Accession No.	3. Recipient's Catalog No.
4. Title and Subtitle SOME FACTORS AFFECTING THE STRESS-CORROSION CRACKING OF Ti-6Al-4V ALLOY IN METHANOL		5. Report Date December 1969
		6. Performing Organization Code
7. Author(s) W. Barry Lisagor		8. Performing Organization Report No. L-6741
		10. Work Unit No. 129-03-21-03-23
9. Performing Organization Name and Address NASA Langley Research Center Hampton, Va. 23365		11. Contract or Grant No.
		13. Type of Report and Period Covered Technical Note
12. Sponsoring Agency Name and Address National Aeronautics and Space Administration Washington, D.C. 20546		
		14. Sponsoring Agency Code

15. Supplementary Notes

16. Abstract

The results of an investigation of factors affecting the stress-corrosion cracking of Ti-6Al-4V alloy in methanol are presented. Both self-stressed and precracked specimens were tested; for the precracked specimens, the analysis was based on fracture mechanics theory. The investigation included the effects of heat treatment, chloride ion content, and presence of initial flaws introduced as fatigue cracks in test specimens. Materials in three heat-treated conditions were included, and chloride ion content varied from 5 to 500 ppm added to the methanol as concentrated hydrochloric acid. Stress levels from 25 to 100 ksi (170 to 690 MN/m^2) were used for self-stressed specimen tests, and initial stress intensities from approximately 4 ksi $(in.)^{1/2}$ (4.4 MN/m^2 $(m)^{1/2}$) to the critical value were used for precracked specimen tests. Comparisons of the variables in the study with respect to self-stressed and precracked specimen testing were made to determine whether environmental effects were more critical during the early or final stages of exposure.

17. Key Words Suggested by Author(s) Stress corrosion Methanol Titanium Flow growth Fracture toughness	18. Distribution Statement Unclassified – Unlimited		
19. Security Classif. (of this report) Unclassified	20. Security Classif. (of this page) Unclassified	21. No. of Pages 43	22. Price* $3.00

*For sale by the Clearinghouse for Federal Scientific and Technical Information
Springfield, Virginia 22151

SOME FACTORS AFFECTING THE STRESS-CORROSION
CRACKING OF Ti-6Al-4V ALLOY IN METHANOL

By W. Barry Lisagor
Langley Research Center

SUMMARY

The stress-corrosion cracking of Ti-6Al-4V alloy in methanol was investigated by using small laboratory-size bent-beam self-stressed specimens and surface precracked tensile specimens under constant load. The alloy was tested in three conditions: annealed, solution-treated, and solution-treated and aged. Tests were conducted at ambient temperature and pressure in reagent methanol (99.9 mol percent pure) and in methanol containing chloride ion concentrations of 5, 10, 100, and 500 ppm added as concentrated hydrochloric acid. Self-stressed specimens were tested with outer fiber stress levels of 25, 50, and 100 ksi (170, 340, and 690 MN/m^2), and precracked specimens were tested with initial stress intensity parameters from 4 ksi $(in.)^{1/2}$ (4.4 MN/m^2 $(m)^{1/2}$) to the critical stress intensity value of the material. In self-stressed specimen tests in reagent methanol, cracks initiated and propagated to failure in as little as 15 hours for solution-treated and aged material with initial outer fiber stresses of 100 ksi (690 MN/m^2). Generally, the solution-treated and aged material had the least resistance to cracking whereas material solution-treated only had the most resistance to cracking. In tests on self-stressed specimens, chloride ion additions from 5 to 500 ppm appeared to decrease cracking time by an order of magnitude as compared with cracking time in reagent methanol, but there seemed to be little difference in cracking time for the range of chloride contents of this investigation. The effect of chloride additions in tests on precracked specimens was not as severe as that on smooth specimens; this result suggests that the effect of chloride additions is more significant in the early stages associated with initiation and slow crack growth. During tests on precracked specimens in reagent methanol with chloride additions, new cracks were observed microscopically to initiate in the vicinity of the primary crack tip in a few minutes after test initiation. The results indicate that constant load tests on precracked specimens in liquid environments provide definitive results more quickly for materials screening purposes than do self-stressed specimen tests.

INTRODUCTION

The Ti-6Al-4V titanium alloy has been used extensively as both a primary load-bearing material and a thin-walled tankage material in numerous aeronautical and aerospace applications. Several attributes make this alloy attractive for such usage. It has a high strength-weight ratio and is relatively inert to chemical reaction with surrounding environments. The alloy is of the beta isomorphous type, and it can be heat-treated to optimize selected mechanical properties critical to particular applications. The mechanism for the high strength which can be developed in the alloy is considered one of precipitation of fine particles of the stable α and β phases at aging temperatures after solution treatment and water quenching to produce metastable α' martensite. (See ref. 1.) The range of temperatures employed in these heat treatments is relatively wide and allows variation of material properties such as strength, elongation, and toughness. The relative chemical inertness of Ti-6Al-4V is attributed to a thin, adherent, self-healing oxide film which titanium alloys develop. This inertness was demonstrated by the resistance of the Ti-6Al-4V alloy to stress-corrosion cracking in boiling 42 percent $MgCl_2$ and boiling 10 percent NaOH solutions. (See ref. 2.)

The attractive properties of this material have resulted in its use in several exacting aeronautical and aerospace applications before material characterization was complete. This use has resulted in some costly systems failures which have been attributed to stress-corrosion cracking. Catastrophic failures have been reported in thin-walled tanks under pressure containing either nitrogen tetroxide (a strong oxidizer) or methanol (a test fluid used to simulate rocket fuel in ground tests). Various investigators have researched and reported the basic incompatibility of the Ti-6Al-4V alloy with nitrogen tetroxide and with methanol. (See, for example, refs. 3 and 4.) When tank failures were reported (ref. 5), the material was in the solution-treated and aged condition; in other laboratory testing (refs. 3 and 5), failures of the alloy in varying conditions have been reported. For the environmental cracking caused by methanol, several investigators (ref. 6) have confirmed the basic incompatibility between methanol and the Ti-6Al-4V alloy. However, in the investigations which utilized various purities of methanol, various material conditions, and specimen geometries, certain combinations of parameters have given contradictory results.

The present study was undertaken to determine cracking conditions under various loadings of both smooth and precracked specimens of Ti-6Al-4V alloy in reagent methanol. The study included tests on cracking in methanol after particular chloride additions, differences in cracking behavior as a function of heat treatment of the alloy, and analyses of the different testing techniques to evaluate methods for indicating material susceptibility.

The cracking behavior is related to the applied stress for the smooth specimen tests and to stress intensity factors for the precracked specimen tests. Stress intensity factors were determined from fracture mechanics theory. (See ref. 7.)

SYMBOLS

The units used for the physical quantities in this paper are given in both the U.S. Customary System of Units and the International System of Units (SI). (See ref. 8.) The conversion factors required for units in the present study are presented in appendix A.

a surface crack depth, in. (m)

c surface half-crack length, outer surface, in. (m)

K_I stress intensity factor calculated from fracture mechanics theory for a surface crack in a plate at any stress, ksi (in.)$^{1/2}$ (MN/m^2 (m)$^{1/2}$)

K_{Ic} plane strain critical stress intensity factor, ksi (in.)$^{1/2}$ (MN/m^2 (m)$^{1/2}$)

K_{Ii} stress intensity factor to which specimen is loaded at initiation of exposure test, ksi (in.)$^{1/2}$ (MN/m^2 (m)$^{1/2}$)

t nominal specimen thickness, in. (m)

α close-packed hexagonal crystal structure of titanium, generally stable at low temperatures

α' metastable phase observed in titanium and produced by selected heat treatments

β body-centered cubic crystal structure of titanium, generally stable at elevated temperatures

σ outer fiber stress, ksi (MN/m^2)

σ_g gross section stress, ksi (MN/m^2)

σ_{tu} tensile ultimate stress, ksi (MN/m^2)

σ_{ty} tensile yield stress, ksi (MN/m^2)

MATERIALS AND SPECIMENS

Materials

Ti-6Al-4V alloy.- The alloy used in this investigation was Ti-6Al-4V rolled sheet nominally 0.040 in. (0.1 cm) thick, obtained from the producer in two conditions. One sheet was obtained in the annealed condition according to producer specifications, and a second sheet was obtained in the solution-treated condition also prepared under producer specification with a solution-treat temperature of 1650° F (1170 K). Material which was to be tested in the solution-treated and aged condition was aged at Langley Research Center in the final specimen configuration at 980° F (800 K) for 4 hours in vacuum. Chemical analysis of the material in each condition tested and mechanical property data for the various conditions, as supplied by the producer, are listed in tables I and II, respectively.

Test liquid.- The test liquid utilized in this investigation was reagent grade methanol, 99.9 mol percent pure. The methanol was procured in quart quantities; spectral emittance and gas chromatographic curves were supplied for each bottle. Concentrated HCl additions were made to introduce quantities of chloride ion varying from 5 to 500 ppm as calculated on a mass basis.

Specimens

Mechanical property specimens.- A tensile specimen of the configuration and dimensions shown in figure 1(a) was used to determine mechanical property data. This specimen was designed with dimensions so that it could be utilized for both mechanical property testing and sustained load exposure in the test media after precracking. All specimens were prepared with the specimen axis in the longitudinal rolling direction. Specimens were prepared with the use of conventional machining techniques; the edges were broken with fine alumina to remove burrs and provide a mild chamfer to the edges.

Bent-beam self-stressed specimens.- Two types of specimens were used for environmental exposure tests. The smooth specimen used was the bent-beam configuration shown in figure 2 and described in reference 9. This specimen configuration was chosen because the design lends itself to the testing of large numbers of specimens with no requirement for loading equipment. The specimen is prepared from strips 0.25 inch (0.64 cm) wide by 4.0 inches (10.2 cm) long. The ends of the strips are preformed as shown in figure 2(a) and then spotwelded together in the self-stressed configuration as shown in figure 2(b). This procedure results in an applied moment at the ends of the specimen which induces a uniform outer fiber stress in each strip. The applied moment and hence the outer fiber stress can be varied by changing the bend angle at the ends of

the strip. Specimens were prepared for this investigation with outer fiber stresses of 25, 50, and 100 ksi (170, 340, and 690 MN/m^2).

Precracked specimens.- The precracked specimens utilized in the environmental tests were prepared by introducing a small part-through crack in the tensile specimens. A small notch was produced in the center of the specimen by electrical discharge machining (EDM) and was extended in fatigue by cantilever bending. The dimensions and placement of the fatigue crack are shown in figure 1. Nominally, the initial crack was 0.175 in. (0.45 cm) long by 0.025 in. (0.063 cm) deep. The outer fiber stress level for crack extension was 50 ksi (340 MN/m^2) as determined by the flexure formula; approximately 75 000 cycles at a rate of 1500 cpm (25 Hz) were required for the desired crack extension. The crack length at the outer fibers was monitored by periodically interrupting the fatigue process and examining the crack at low magnification. After final preparation and prior to exposure in the test media, all specimens were chemically cleaned by using the procedures described in reference 10.

EQUIPMENT AND PROCEDURES

Mechanical Property Tests

A hydraulic testing machine was used to determine the mechanical properties of the material in each condition. Conventional stress-strain curves were obtained by use of microformer-type extensometers to determine strain which was autographically plotted against stress by utilizing an x,y recorder. Specimens tested for tensile ultimate and yield strengths were tested at a strain rate of 0.005 per minute to yield strength and 0.05 per minute to ultimate strength.

Environmental Exposure Tests

Bent-beam self-stressed specimens.- Before exposure in the test media, the ends of the specimens were coated with wax to prevent attack in the area of the bend angle where a stress concentration existed. The specimens were then immersed in the test media in glass beakers which were sealed with a plastic cover after immersion to prevent the methanol from absorbing water from the laboratory atmosphere during the exposure test. The laboratory atmosphere was maintained at a nominal temperature of 80° F (300 K) and a nominal relative humidity of 50 percent before sealing. These specimens were immersed for 30 minutes to 500 hours and observed periodically for evidence of cracking. Rapid failure occurred after cracks appeared. When failures occurred, test duration time was recorded. If a specimen did not show visual evidence of cracking after a predetermined test duration, it was removed and tested in axial compression. If small cracks were present, they would be opened by the axial loading, and

would thus allow visual observation of cracking severity. Metallurgical examinations were made on selected specimens after exposure. It should be noted that this type of specimen was exposed after stressing in contrast to the normal service procedures for aircraft and spacecraft tankage which are filled and then stressed by pressurization.

Tensile precracked specimens.- Tensile precracked specimens were tested in a static loading frame equipped with a stage micrometer and microscope so that surface crack behavior could be observed during testing. The testing machine (fig. 3) was similar in design to apparatus described in reference 11. The specimen was supported horizontally and was insulated electrically from the test frame by steel loading pins which had been flame sprayed with high purity alumina. The container for the test media was constructed of Ti-6Al-4V alloy and painted with an epoxy-resin. The loading instrumentation was calibrated just prior to each test, and the loading frame was capable of applying tensile loads to 2000 lbf (8.88 kN). Nominal loads were maintained with an accuracy of approximately ±10 pounds (±44 N). Specimens were tested in this apparatus for a maximum of 6 to 8 hours because the solution was not covered to prevent water pickup. Nominal laboratory atmospheric conditions were the same as those for the self-stressed specimens. A typical test sequence consisted of positioning the specimen in the loading frame and preloading to determine the approximate crack length. This crack length was used to estimate the initial stress intensity factor K_{Ii} for the test. Details of the stress intensity factor K_I calculation are described in appendix B. Specimens were unloaded before the container was filled with the test liquid; the specimens were again loaded to the desired target stress intensity. During the exposure, the crack tip areas were observed through the microscope, and cracking behavior was characterized by use of photomicrography to observe changes in cracking conditions. Constant load was applied until the specimen failed or the test was terminated. If the specimen failed, the fracture surface was examined and the initial crack dimensions were measured with a filar micrometer eyepiece. These initial crack dimensions were used to recalculate K_{Ii} values. The fracture surface was also examined to determine the magnitude of crack growth preceding fast fracture. If the specimen did not fail during exposure, it was tested in tension to failure. The fracture surface was subsequently examined for measurement of initial crack dimensions and for evidence of crack extension during exposure.

Metallurgical Examination

Specimens of the Ti-6Al-4V material as received and after laboratory heat treatment were prepared for observation by using standard metallographic techniques to characterize the microstructure of the materials. Kroll's etchant (2 parts concentrated HNO_3, 1 part concentrated HF, 97 parts H_2O) was utilized for all material conditions.

Typical photomicrographs of the material in each condition are shown in figure 4. Electron probe X-ray microanalysis was employed to provide concentration profiles of the primary alloying elements. Similar analyses were made on specimens which had failed as a result of the exposure test to determine element concentration profile near the fracture surface. To more fully characterize the microstructure, X-ray diffraction patterns were obtained from tensile specimens of the material in each condition. Patterns were obtained by using Cu Kα radiation at an accelerating voltage of 40 kV. The X-ray detector utilized was a scintillation counter, and pulse-height discrimination was employed to alleviate the fluorescence problem common to titanium and titanium alloys.

RESULTS AND DISCUSSION

Mechanical and Metallurgical Properties of Ti-6Al-4V

The mechanical property data determined from this investigation are in reasonable agreement with the data provided by the manufacturer; both are shown in table II. All values reported in this investigation represent an average value for two tests and very little scatter was observed when duplicate tests were performed. Fracture toughness tests conducted in this investigation utilizing the surface-cracked tensile specimens yielded the K_{Ic} results presented in table II. Appendix C contains a detailed discussion of the metallographic data of figure 4 in addition to discussions of the X-ray diffraction data (table III) and electron probe results.

Bent-Beam Specimen Environmental Exposure Testing

A complete listing of environmental exposure test results for the bent-beam self-stressed specimens is given in table IV. Effects of specific factors which appear to be significant are discussed in the following paragraphs.

Effect of applied stress.- Specimens in the annealed condition which were stressed to 100 ksi (690 MN/m^2) had an average time to failure of 67 hours when exposed in reagent grade methanol. This time to failure represents both initiation and growth of cracks until complete fracture of the specimen occurred. There was considerable variation in the time to failure of duplicate specimens. If a sufficient number of cracks initiate in this type of specimen, the stress intensity factor for each crack tip may be lower. Because of this effect, variations in the number of cracks initiated may result in varying crack growth rates and hence different failure times. Specimens which were tested with outer fiber stresses of 50 and 25 ksi (340 and 170 MN/m^2) contained deep cracks after 500 hours exposure but did not fracture. Self-stressed specimens after fabrication and various stages of testing are shown in figure 5. Figure 5(a) illustrates a specimen as fabricated with an outer fiber stress of 100 ksi (690 MN/m^2). A 100 ksi

7

(690 MN/m^2) specimen which fractured during exposure is shown in figure 5(b), and 50 and 25 ksi (340 and 170 MN/m^2) specimens which contained cracks after 500 hours exposure are shown in figures 5(c) and 5(d), respectively. These specimens are shown in figure 6 at low magnification to illustrate the effectiveness of the compression test in opening the cracks for observation. Visual inspection at low magnification before compression testing did not reveal the presence of the cracks.

Effect of chloride ion addition.- The effect of small chloride ion additions to the methanol on the failure time of annealed specimens stressed to 100 ksi (690 MN/m^2) is illustrated in figure 7. The time to failure is reduced by an order of magnitude by additions of chloride ion of 5 ppm or greater. No appreciable difference in behavior in solutions containing 5 ppm or 500 ppm or levels between these values was observed. This behavior suggests that a regenerative reaction may be occurring which requires only a small concentration of chloride ion to continue the process.

Effect of material condition.- The times to failure of specimens in each material condition after exposure in reagent methanol and methanol containing 100 ppm chloride ion are shown in figure 8 and table IV. All specimens were stressed to outer fiber levels of 100 ksi (690 MN/m^2). For exposure in reagent methanol, the material was susceptible to cracking in each condition, but the average time to failure varied somewhat. The aged material in the highest strength condition exhibited the shortest average time to failure whereas the material in the solution-treated condition exhibited the longest time to failure. The same general trend was observed for tests in solutions containing 100 ppm chloride ion. The drastic shortening of failure time in solutions containing chloride ion was observed for all material conditions. (See fig. 8.) The results of all tests conducted on the bent-beam specimen are summarized in table IV.

Precracked Specimen Environmental Exposure Testing

The effects of specific factors on the behavior of the precracked specimens in the environmental exposure tests are discussed in the following paragraphs and are summarized in table IV.

Environmental cracking in reagent methanol.- The results of the environmental cracking tests on material in each condition are shown in figure 9. The data shown at zero time represent the critical stress intensity factor K_{Ic} for specimens tested in air. The solution-treated material appeared to have the greatest resistance to crack growth. For initial stress intensities of approximately half the critical stress intensity, specimens in all material conditions failed in less than 2 hours. The curves tend to level off rapidly and approach a lower level of initial stress intensity below which crack growth was not observed in the length of exposures utilized in this investigation. The time to

failure for material in the solution-treated and aged condition is in excellent agreement with the results indicated in reference 12 for exposure in reagent methanol. In addition, comparison of these results with those of references 12 and 13 indicates that the cracking of Ti-6Al-4V is more severe in reagent methanol than in water or salt solution.

A sequence of photomicrographs of an annealed specimen under test is shown in figure 10. The pictures illustrate the appearance of the specimen surface at one end of the crack. The initial indication of crack growth was generally observed as an opening of the existing initial crack before extension occurred on the surface of the specimen. The observed opening is attributed to initial crack growth at the base of the crack where the stress intensity for a semielliptical defect is the greatest. This area was within the specimen and could not be observed directly. Extension at the outer surface subsequently occurred and the crack-length extension could be observed to failure. In tests conducted in reagent methanol, the attack appeared to be confined to the initial defect, although the crack showed some tendency to fork at the tip and then extend selectively in one of the branches. (See figs. 10(c) and 10(d).) Figure 11 shows the cross section of the failure after test. The initial flaw, environmental crack extension, and fast fracture regions are clearly visible and are labeled. The illustrations in figures 10 and 11 are characteristic of the results obtained for all three material conditions tested in reagent methanol. These tests indicate that the precracked specimen configuration can be used effectively for materials screening. Using precracked specimens instead of self-stressed specimens will reduce test duration. From these tests and from the tests on self-stressed specimens in reagent methanol, there appears to be a basic incompatibility between the Ti-6Al-4V alloy and the methanol as commercially produced.

Environmental cracking in methanol containing chloride ions.- The results of tests on precracked specimens exposed in methanol containing 100 ppm chloride ion are shown in figure 12. The curve in figure 12 for a given material condition tends toward a lower threshold stress intensity parameter than is indicated in tests without chloride ion additions (fig. 9). The effect of material condition on cracking behavior is shown in figure 13. A comparison of these data indicates that the addition of the chloride ions in this small concentration lowered the times to failure by a factor of about three. The fact that the chloride ion addition had a more severe effect on time to failure for self-stressed tests (fig. 8) than for precracked specimen tests (fig. 13) indicates that the ion plays a larger role in initiation and early growth than in later crack extension prior to failure. This result is further substantiated by a comparison of the series of photomicrographs in figures 10 and 14. Figure 14 shows one end of the crack in a solution-treated specimen during exposure in methanol containing chloride ion. The behavior is similar to the extension observed in reagent methanol but more rapid. However, after approximately 20 minutes exposure, additional cracks appeared to initiate in the area of the crack tip

prior to failure. These cracks appear to be newly initiated ones rather than branches or tunnels from the primary crack. Note in figure 10 that after 44 minutes exposure in reagent methanol, no new cracks were observed. The fracture surface of the specimen of figure 14 is shown in figure 15 with characteristic fracture areas identified.

General Discussion

The results of precracked exposure tests shown in figures 9 and 12 indicate the solution-treated material to be somewhat more resistant to the environmental cracking than either the annealed or solution-treated and aged conditions. The same trend was indicated by the smooth specimen tests. However, the fact that annealed material performed as well or better than the aged material suggests the cracking is a function of not only fracture toughness but also a combination of material properties. The material in the aged condition is less ductile; the higher degree of elastic constraint along the crack front and the decrease in ductility may contribute significantly to the material susceptibility.

Although the threshold stress intensity required to extend a defect in a given environment appears to be rapidly approached in exposure tests, as indicated in figures 9 and 12 and in reference 12, the test duration for establishing the threshold must not be arbitrarily chosen. Too short an exposure time may lead to unconservative predictions. For example, reference 12 reports a threshold stress intensity of approximately 11 ksi (in.)$^{1/2}$ (121 MN/m^2 (m)$^{1/2}$) for material in the solution-treated and aged condition exposed in reagent methanol. This threshold was based on a maximum exposure time of 48 hours for forged material. According to this threshold, a surface crack size of approximately 0.004 in. (0.01 cm) deep by 0.020 in. (0.051 cm) long could be tolerated in 0.040 in. (0.1 cm) material stressed to 100 ksi (690 MN/m^2) before subcritical crack growth would occur. Stress-corrosion failures in this investigation were observed in all self-stressed specimens tested at 100 ksi (690 MN/m^2), although visual examination at low magnification did not reveal the existence of initial flaws of this size. Apparently, initial exposure behavior in the presence of very small defects does not adhere strictly to flaw-growth theory utilizing precracked specimens. Increased electrochemical action may cause small defects to extend in early stages, perhaps because of a pitting corrosion phenomenon.

An alternate approach might be based on the rate of crack growth for different flaw sizes, these rates being taken into consideration when applications of long duration are designed. In this manner actual exposure times for application might be safely predicted with tests of duration shorter than actual service. An approach of this type would apply essentially to environmental flaw growth under constant load as experienced in various pressure vessel applications.

10

CONCLUSIONS

An investigation was undertaken to determine the effects of material condition, impurity levels of chloride ion, and various loading techniques on the stress-corrosion cracking of Ti-6Al-4V alloy in methanol. The following conclusions are based on the results of the investigation:

1. The stress-corrosion cracking of the Ti-6Al-4V alloy in methanol appears to result from a basic incompatibility between the materials and may be governed by certain impurities in the methanol which could be present in nearly undetectable concentrations. Chloride ions added as HCl in small concentrations reduce the time to failure. The effect of the chloride appears to be more significant during early stages of cracking than during later stages. The effect is severe and indicates that control tests utilizing the liquid to be used in service hardware are needed to insure confidence that environmental factors will not cause service failures.

2. The resistance to crack extension in the presence of the corrodent appears to be dependent on but not limited to the fracture toughness condition of the material. The degree of ductility and, in particular, local deformation near crack fronts may have more effect on environmental flaw growth than on critical stress intensity factor determinations.

3. The precracked specimen approach appears to be a desirable method for rapid screening of materials with respect to stress-corrosion cracking in liquids. However, in utilizing the precracked specimen approach for design purposes, the true threshold stress intensity level should be determined for the environment and exposure time to be encountered in application.

Langley Research Center,
National Aeronautics and Space Administration,
Langley Station, Hampton, Va., August 22, 1969.

APPENDIX A

CONVERSION OF U.S. CUSTOMARY UNITS TO SI UNITS

The International System of Units (SI) was adopted by the Eleventh General Conference on Weights and Measures in 1960 (ref. 8). Conversion factors for the units used herein are given in the following table:

Physical quantity	U.S. Customary Unit	Conversion factor (a)	SI Unit (b)
Force	lbf	4.448	newton (N)
Frequency	cycles/minute	0.0167	Hertz (Hz)
Length	in.	0.0254	meter (m)
Stress	$psi = lbf/in^2$	6895	$newton/meter^2$ (N/m^2)
Stress intensity	$ksi (in.)^{1/2}$	1.099	$MN/m^2 (m)^{1/2}$
Temperature	$(^oF + 460)$	5/9	Kelvin (K)

[a]Multiply value given in U.S. Customary Units by conversion factor to obtain equivalent value in SI Unit.

[b]Prefixes to indicate multiple of units are as follows:

Prefix	Multiple
nano (n)	10^{-9}
micro (μ)	10^{-6}
milli (m)	10^{-3}
centi (c)	10^{-2}
kilo (k)	10^3
mega (M)	10^6

DETERMINATION OF STRESS INTENSITY FACTORS

FOR SURFACE CRACKS

Development of Stress Intensity Solution

The equation used for the calculation of the stress intensity in this investigation was first developed by Irwin (ref. 7), and later modified by Kobayashi (ref. 14) and is as follows:

$$K = 1.1 M_{kf} M_{kp} (\pi)^{1/2} \frac{\sigma_g}{(c)^{1/2}} \left(\frac{a}{Q}\right)^{1/2} \left(a^2 \cos^2 \varphi + c^2 \sin^2 \varphi\right)^{1/4} \tag{1}$$

where

a   crack depth

c   surface half-crack length

K   stress intensity factor for any point along crack front as illustrated in figure 16

M_{kf} magnification of stress intensity for a deep flaw in an infinite strip

M_{kp} magnification of stress intensity due to plastic yielding in an infinite plane

$$Q = \left[\int_0^{\pi/2} \left(1 - \frac{c^2 - a^2}{c^2} \sin^2 \theta \right)^{1/2} d\theta \right]^2$$

θ dummy variable for integration

σ_g gross area stress

φ angle between major axis of ellipse and line drawn from center of ellipse to any point along crack front at which value of K is desired (fig. 16)

The maximum value of K occurs along the minor axis of the ellipse. At that point, equation (1) reduces to

$$K = 1.1 M_{kf} M_{kp} \sigma_g \left(\frac{\pi a}{Q}\right)^{1/2} \tag{2}$$

In reference 15, M_{kf} was expressed as $\beta^{1/2}$ and determined by

$$M_{kf} \equiv (\beta)^{1/2} = \left[4 \sum_{n=1}^{\infty} n F_O^{(2n)} (a/t)^{2n-2}\right]^{1/4} \tag{3}$$

The values for $F_O^{(2n)}$ for the first six terms of the summation (n = 1,2,3,4,5,6) are -0.2500, -0.148710, -0.109687, -0.085314, -0.068697, and -0.06156.

As used in reference 14, M_{kp} is determined by

$$M_{kp} = \left[\frac{Y}{\sigma_g} \frac{1}{\pi} \log_e \frac{1 + \sin\left(M_{kf} \frac{\sigma_g}{Y} \frac{\pi}{2}\right)}{1 - \sin\left(M_{kf} \frac{\sigma_g}{Y} \frac{\pi}{2}\right)}\right]^{1/2} \tag{4}$$

where Y, the equivalent stress, is given by $Y = \dfrac{\sigma_{ty} - \nu\sigma_g}{1 - 2\nu}$ and ν is the Poisson's ratio of the material.

Equations (1) to (4) were utilized in a computer program with inputs of material yield stress, applied load, Poisson's ratio, dimensions of specimen thickness and width, and crack length and depth for calculation of applied or critical K values. A source listing and sample data for a typical calculation is given at the end of this appendix.

Initial Fracture Toughness Determinations

The values for K_{Ic}, the critical stress intensity factor, calculated from equation (2) for material in the annealed condition are shown in figure 17. It is generally considered that the critical stress intensity factor determined from tests of specimens under plane strain conditions is constant for a given material in a given condition. Thus, K_{Ic} is independent of the type of specimen utilized as long as specimen dimensions insure plane strain conditions. For this investigation, it was necessary to determine whether valid predictions could be made by using specimens which had a nominal thickness of 0.040 in. (0.1 cm). Figure 17 shows calculated K_{Ic} values and the ratio of gross failure stress to material yield stress as a function of the ratio of crack depth to specimen thickness. If the solution as developed was valid for any crack size in the chosen configuration, then the value for K_{Ic} in figure 17 would be a horizontal straight line. The values for K_{Ic} of figure 17 agree very well with literature values (ref. 16)

14

for a/t ratios above 0.65. Cracks of this depth or greater resulted in failure stresses below 85 percent of yield stress. With smaller crack depths where failure stress exceeded 85 percent of yield stress, the apparent stress intensity values drop below the constant K_{Ic} level. As a result, the solution appears to be inadequate for small cracks in Ti-6Al-4V annealed material in this nominal thickness. Consequently, initial crack depths for this study were maintained between 0.65 and 0.75 of nominal material thickness.

The details of the fracture surface of a typical specimen from which the data of figure 17 were determined are shown in figure 18. The initial crack does appear to be semielliptical. From the fracture appearance, the crack seems to extend in cleavage a very short distance from the fatigue front before ultimate failure in shear. The area labeled fast fracture in figure 18 includes both the cleavage and shear regions.

The results of the fracture toughness tests on specimens in each material condition indicated the solution-treated condition to be the toughest with a K_{Ic} average of 56.9 ksi (in.)$^{1/2}$ (62 MN/m^2 (m)$^{1/2}$. The critical stress intensity factors for material in the annealed and the solution-treated and aged condition were 45.5 and 51.6 ksi (in.)$^{1/2}$ (50 and 57 MN/m^2 (m)$^{1/2}$), respectively. These values represent an average of several tests in each condition. Very little scatter was observed in the duplicate tests. The results indicate that the solution-treated condition might be a better choice for application where toughness is considered an important design criterion.

Source Listing and Sample Data for Automated

Calculation of K Values

The source listing and sample data for calculation of K values follows:

```
      PROGRAM SURFLAW (INPUT,OUTPUT)
      DIMENSION RESULT(2),AREA(50),TWOC(50),A(50),PMAX(50),THCKS(50),
     1WDTHS(50),SIGYS(50),SUM(1),FOFX(1)
      REAL NU,K,MKF,MKP,K1
      EXTERNAL FUNC
      COMMON CC,AA
      NAMELIST/CRKGEOM/NSPEC,AREA,TWOC,A,PMAX,THCKS,WDTHS,ICAREA,
     1SIGYS,NU,NSIGYS
    1 CALL DAYTIM (RESULT)
      PRINT 2, RESULT
    2 FORMAT(*1DATE*3XA10,5X*TIME*3XA10/
     1* DETERMINATION OF MODE STRESS INTENSITY PARAMETERS*/
     2* FOR SURFACE FLAWED TENSILE SPECIMENS*/
     3* ROBINSON-LISAGOR, SPD-A2241, RDB-225, JUNE 1968*)
      PI=3.14159265358979
C READ INPUT DATA
      READ CRKGEOM
      DO 7 I=1,NSIGYS
      DO 7 J=1,NSPEC
      IF (ICAREA.EQ.1) GO TO 3
```

APPENDIX B

```
CALCULATE WIDTH IF AREA AND THICKNESS ARE GIVEN
      WDTHS(J)=AREA(J)/THCKS(J)
      GO TO 4
CALCULATE AREA IF WIDTH AND THICKNESS ARE GIVEN
    3 AREA(J)=WDTHS(J)*THCKS(J)
    4 PRINT 5, THCKS(J),WDTHS(J),AREA(J),TWOC(J),A(J),PMAX(J),SIGYS(I),
     1NU
    5 FORMAT(////* CRACK GEOMETRY*/5X*THICKNESS OF SPECIMEN =*F9.5/
     19X*WIDTH OF SPECIMEN =*F9.5/22X*AREA =*F9.5/
     211X*LENGTH OF CRACK =*F9.5/12X*DEPTH OF CRACK =*F9.5/
     314X*MAXIMUM LOAD =*F9.1/12X*YIELD STRENGTH =*F9.1/
     412X*POISSONS RATIO =*F9.5)
C FAILING OR INITIAL LOAD APPLIED
      SIGMA=PMAX(J)/AREA(J)
CRACK DEPTH TO THICKNESS RATIO
      K=A(J)/THCKS(J)
      BETA=SQRT(4.*(.25+.29742*K**2+.329061*K**4+.341256*K**6+.343485*
     1K**8+.36936*K**10))
C MAGNIFICATION DUE TO FINITE DIMENSIONS
      MKF=SQRT(BETA)
      Y=(SIGYS(I)-NU*SIGMA)/(1.-2.*NU)
C MAGNIFICATION DUE TO PLASTIC YIELDING
      SARG=SIN(MKF*SIGMA*PI/(Y*2.))
      MKP=SQRT(Y*ALOG((1.+SARG)/(1.-SARG))/(SIGMA*PI))
C FLAW SHAPE PARAMETER
      CC=TWOC(J)/2.
      AA=A(J)
      UP=PI/2.
      CALL MGAUSS (0.,UP,10,SUM,FUNC,FOFX,1)
      PHI=SUM(1)
      Q=PHI**2
C OPEN MODE STRESS INTENSITY PARAMETER
      K1=1.1*MKF*MKP*SQRT(PI)*SIGMA*SQRT(A(J)/Q)
C PRINT OUTPUT
      PRINT 6, SIGMA,K,MKF,MKP,Q,K1
    6 FORMAT(/* OUTPUT DATA*/5X*SIGMA =*E15.8/9X*K =*E15.8/
     17X*MKF =*E15.8/7X*MKP =*E15.8/9X*Q =*E15.8/8X*K1 =*E15.8//)
    7 CONTINUE
      GO TO 1
      END
      SUBROUTINE FUNC (X,FOFX)
      DIMENSION FOFX(1)
      COMMON CC,AA
      TERM=(CC**2-AA**2)/CC**2
      FOFX(1)=SQRT(1.0-TERM*SIN(X)**2)
      RETURN
      END
```

```
CRACK GEOMETRY
     THICKNESS OF SPECIMEN =    .04415
         WIDTH OF SPECIMEN =    .50370
                     AREA =     .02224
          LENGTH OF CRACK =     .19330
           DEPTH OF CRACK =     .02970
             MAXIMUM LOAD =    2455.0
           YIELD STRENGTH = 133500.0
           POISSONS RATIO =    .30000
OUTPUT DATA
     SIGMA = 1.10394856E+05
         K = 6.72706682E-01
       MKF = 1.19218109E+00
       MKP = 1.16432748E+00
         Q = 1.21039887E+00
        K1 = 4.68002102E+04
```

APPENDIX C

METALLURGICAL EXAMINATION

Metallographic Investigation

The microstructure of the Ti-6Al-4V alloy in each test condition is shown in figure 4. The annealed material shown in figure 4(a) consists primarily of α phase with a small percentage of β phase present as a result of the equilibrium conditions associated with the annealing temperature. The microstructure of material solution-treated at 1650° F (1170 K) shown in figure 4(b) consists of primary α grains in a matrix of transformed material α' as a result of the rapid quench. The microstructure after aging at 980° F (800 K) for 4 hours is shown in figure 4(c). The transformed structure appears to have begun precipitation of fine particles tending toward equilibrium. The appearance of this microstructure and the results of the mechanical property tests indicate that the material is in the desired high-strength condition for the particular solution-treat temperature employed.

X-ray and Electron Probe Investigation

The results of the X-ray diffraction analysis on the material conditions tested are given in table III. The results substantiate the phases in the observed microstructures (fig. 4). Analysis on material in the annealed condition revealed reflections of both α and β phases. Comparison of the observed microstructure with ASTM data indicated that the solute concentration had little effect on the interplanar spacing in the α phase; however, the interplanar spacing in the β phase differed from the observed values for the Ti-8Al-1Mo-1V material used in reference 17. The solution treatment decreases the relative amount of β stabilizers in the β phase, and the subsequent quench results in the transformation of the β phase which contains too low a concentration of stabilizing elements to persist at the lower temperatures. There were no discernible β reflections on the diffraction patterns of solution-treated and quenched material. Also of interest was the apparent lack of change in interplanar spacing of transformed material compared with α phase spacing; neither were mechanical properties drastically changed. The diffraction patterns obtained after aging indicate a tendency to precipitate β phase as evidenced by the slight reflection of the 211 planes in the β phase. This reflection was also the strongest intensity reflection of β phase in the annealed material.

The relative intensities of the reflections observed indicate some degree of preferred orientation commonly observed in rolled sheet. The same general trend of orientation texturing was observed for the material in each condition investigated.

APPENDIX C

Electron-probe X-ray microanalyzer traces across metallographic sections of the alloy in each condition indicated uniform concentrations of the primary elements present (Ti, Al, and V). However, the X-ray resolution associated with probe analysis is at best 2 to 5 microns (2 to 5 μm) which borders on the apparent particle size of β phase (fig. 4(a)) and may prevent identification of higher concentrations of β stabilizers in this phase. Concentration profiles adjacent to the fracture surfaces of specimens which failed during the environmental exposure indicated no appreciable concentration change in the primary elements.

REFERENCES

1. Comerford, M. F.; Averbach, B. L.; and Bever, M. B.: Physical Metallurgy of Titanium Alloys. Tech. Rep. No. 1 (Contract Nonr-1841(02)), Massachusetts Inst. Technol., Jan. 31, 1958.

2. Anon.: Titanium for the Chemical Engineer. DMIC Mem. 234, Battelle Mem. Inst., Apr. 1, 1968.

3. Lisagor, W. Barry; Manning, Charles R., Jr.; and Bales, Thomas T.: Stress-Corrosion Cracking of Ti-6Al-4V Titanium Alloy in Nitrogen Tetroxide. NASA TN D-4289, 1968.

4. Johnston, Robert L.; Johnson, Robert E.; Ecord, Glenn M.; and Castner, Willard L.: Stress-Corrosion Cracking of Ti-6Al-4V Alloy in Methanol. NASA TN D-3868, 1967.

5. Kappelt, G. F.; and King, E. J.: Observations on the Stress Corrosion of the 6Al-4V Titanium Alloy in Nitrogen Tetroxide. Rep. No. AFML-TR-67-329, Part 1, U.S. Air Force, Nov. 1967, pp. 922-941.

6. Anon.: Accelerated Crack Propagation of Titanium by Methanol, Halogenated Hydrocarbons, and Other Solutions. DMIC Mem. 228, Battelle Mem. Inst., Mar. 6, 1967.

7. Irwin, G. R.: Crack-Extension Force for a Part-Through Crack in a Plate. Trans. ASME, Ser. E.: J. Appl. Mech., vol. 29, no. 4, Dec. 1962, pp. 651-654.

8. Comm. on Metric Pract.: ASTM Metric Practice Guide. NBS Handbook 102, U.S. Dep. Com., Mar. 10, 1967.

9. Heimerl, George J.; and Braski, D. N.: A Stress Corrosion Test for Structural Sheet Materials. Mater. Res. Stand., vol. 5, no. 1, Jan. 1965, pp. 18-22.

10. Heimerl, George J.; Baucom, Robert M.; Manning, Charles R., Jr.; and Braski, David N.: Stability of Four Titanium-Alloy and Four Stainless-Steel Sheet Materials After Exposures up to 22 000 Hours at 550° F (561° K). NASA TN D-2607, 1965.

11. Ryabchenkov, A. V.; and Nikiforova, V. M.: Role of Electrochemical Factors in the Process of Corrosion Cracking of Austenitic Steels. Intercrystalline Corrosion and Corrosion of Metals Under Stress, I. A. Levin, ed., Consultants Bureau Enterprises, Inc., 1962, pp. 161-178.

12. Tiffany, C. F.; and Masters, J. N.: Investigation of the Flaw Growth Characteristics of 6Al-4V Titanium Used in Apollo Spacecraft Pressure Vessels. NASA CR-65586, 1967.

13. Figge, I. E.; and Hudson, C. Michael: Crack Propagation, Delayed Failure, and Residual Static Strength of Titanium, Aluminum, and Stainless Steel Alloys in Aqueous Environments. NASA TN D-3825, 1967.

14. Tiffany, C. F.; Lorenz, P. M.; and Shah, R. C.: Extended Loading of Cryogenic Tanks. NASA CR-72252, 1966.

15. Forman, R. G.; and Kobayashi, A. S.: On the Axial Rigidity of a Perforated Strip and the Strain Energy Release Rate in a Centrally Notched Strip Subjected to Uniaxial Tension. Trans. ASME, Ser. D.: J. Basic Eng., vol. 86, no. 4, Dec. 1964, pp. 693-699.

16. Steigerwald, E. A.: Plane Strain Fracture Toughness Data for Handbook Presentation. Rep. No. AFML-TR-67-187, U.S. Air Force, July 1967. (Available from DDC as AD821626.)

17. Pride, Richard A.; Royster, Dick M.; Stein, Bland A.; and Gardner, James E.: Effects of Longtime Environmental Exposure on Mechanical Properties of Sheet Materials for a Supersonic Transport. NASA TN D-4318, 1968.

TABLE I.- CHEMICAL ANALYSES OF Ti-6Al-4V[a] SHEET

Condition	Producer analysis, percent by weight							
	C	Fe	N	Al	V	H_2	O_2	Ti
Annealed	0.025	0.05	0.015	5.9	4.1	0.008	0.11	Balance
Solution-treated	.023	.07	.011	5.9	4.0	.010	.12	Balance
Solution-treated, aged	.023	.07	.011	5.9	4.0	.010	.12	Balance

[a]Nominal thickness, 0.040 in. (0.1 cm).

TABLE II.- MECHANICAL PROPERTIES OF Ti-6Al-4V SHEET

Condition	This investigation[a]									Producer reported				
	σ_{tu}		σ_{ty}		Elongation		K_{Ic}			σ_{tu}		σ_{ty}		Elongation, percent in 2 in.
	ksi	MN/m²	ksi	MN/m²	Percent in 1 in.	Percent in 2 in.	ksi (in.)¹/²	MN/m² (m)¹/²		ksi	MN/m²	ksi	MN/m²	
Annealed	143.0	985.0	133.5	920	17	12.5	45.5	50		139.7	950	135.5	935	12.5
Solution-treated[b]	152.5	1050	134.5	925	13	9	56.9	62.5		155.2	1070	139.5	960	11.0
Solution-treated, aged[c]	164.5	1130	150.5	1040	11	8	51.6	57		167.3	1150	154.4	1060	10.0

[a]Values reported are average values of all tests.
[b]Solution treat temperature, 1650° F (1170 F).
[c]Producer aging treatment, 4 hours at 1000° F (810 K). Aging treatment for this investigation, 4 hours at 980° F (790 K).

TABLE III.- X-RAY DIFFRACTION IDENTIFICATION OF PHASES OBSERVED IN Ti-6Al-4V SHEET

Miller indices, hkl		Pure titanium ASTM 5-0682			Ti-6Al-4V annealed			Ti-6Al-4V solution-treated			Ti-6Al-4V solution-treated, aged		
α	β	Interplanar spacing		Relative intensity normalized to strongest reflection	Interplanar spacing		Relative intensity normalized to strongest reflection	Interplanar spacing		Relative intensity normalized to strongest reflection	Interplanar spacing		Relative intensity normalized to strongest reflection
		Å	nm		Å	nm		Å	nm		Å	nm	
100		2.557	0.2557	30	2.546	0.2546	83	2.540	0.2540	60	2.543	0.2543	100
002		2.342	.2342	26	2.343	.2343	66	2.342	.2342	60	2.343	.2343	78
101		2.244	.2244	100	2.232	.2232	100	2.231	.2231	73	2.233	.2233	86
102		1.726	.1726	19	1.719	.1719	43	1.723	.1723	53	1.720	.1720	46
110		1.475	.1475	17	1.464	.1464	36	1.464	.1464	84	1.464	.1464	55
103		1.332	.1332	16	1.326	.1326	70	1.326	.1326	100	1.327	.1327	96
200		1.276	.1276	2	1.267	.1267	17	1.267	.1267	14	1.268	.1268	17
112		1.247	.1247	16	1.240	.1240	42	1.241	.1241	43	1.240	.1240	51
201		1.233	.1233	13	1.223	.1223	30	1.224	.1224	27	1.223	.1223	25
	110				2.270	.2270	10						
	200				1.599	.1599	8						
	211				1.307	.1307	12				1.301	.1301	7

Condition	σ		K_{Ii}		Chloride additions, ppm (a)	Exposure time, hr	Type of failure	Remarks
	ksi	MN/m²	ksi (in.)$^{1/2}$	MN/m² (m)$^{1/2}$				
Self-stressed specimens								
Annealed	100	690	----	----	0	153	Fracture	
			----	----	0	100		
			----	----	0	69		
			----	----	0	57		
			----	----	0	37		
			----	----	0	32		
			----	----	0	23	↓	
	50	345	----	----	0	500	Change in relative deflection upon compression	Surface cracks observed
	25	170	----	----	0	500		
Solution-treated	100	690	----	----	0	48	Fracture	
			----	----	0	64		
			----	----	0	68		
			----	----	0	72		
			----	----	0	110		
			----	----	0	132		
			----	----	0	140		
Solution-treated, aged			----	----	0	16		
			----	----	0	16		
			----	----	0	63		
			----	----	0	69		
Annealed			----	----	5	10		
			----	----	10	1.2		
			----	----	100	8		
			----	----	100	6		
			----	----	100	1.0		
			----	----	100	.8		
Solution-treated			----	----	100	16		
			----	----	100	27		
			----	----	100	16		
Solution-treated, aged			----	----	100	1		
			----	----	100	4		
Annealed			----	----	500	5		
			----	----	500	4	↓	

aChloride added as concentrated HCl.

TABLE IV.- SUMMARY OF ENVIRONMENTAL EXPOSURE TESTS IN REAGENT METHANOL WITH OR WITHOUT CHLORIDE ADDITIONS – Concluded

Condition	σ		K_{Ii}		Chloride additions, ppm (a)	Exposure time, hr	Type of failure	Remarks
	ksi	MN/m²	ksi (in.)$^{1/2}$	MN/m² (m)$^{1/2}$				
Precracked tensile specimens								
Annealed	---	---	24.1	26.5	0	1.41	Fracture	
Solution-treated	---	---	27.3	30.0	0	1.83	↓	
Solution-treated, aged	---	---	26.0	28.6	0	1.07	↓	
Annealed	---	---	16.7	18.3	0	6.90	None	No crack growth observed
Solution-treated	---	---	16.2	17.8	0	6.65	↓	
Solution-treated, aged	---	---	17.3	19.0	0	6.40	↓	
Annealed	---	---	24.5	26.9	100	.284	Fracture	
Solution-treated	---	---	26.6	29.1	100	.67	↓	
Solution-treated, aged	---	---	25.7	28.2	100	.350	↓	
Annealed	---	---	15.5	17.0	100	.615	↓	
Solution-treated	---	---	17.1	18.8	100	2.32	↓	
Solution-treated, aged	---	---	16.2	17.8	100	.650	↓	
Annealed	---	---	8.85	9.73	100	7.75	None	No crack growth observed
Solution-treated	---	---	7.54	8.3	100	8	↓	Surface crack length increase observed during exposure, crack growth observed after tensile test
Solution-treated, aged	---	---	8.31	9.13	100	3.62	Fracture	
	---	---	4.51	4.95		7.85	None	No crack growth observed

^{a}Chloride added as concentrated HCl.

Diam. = 0.5
(1.3)

Crack location of
precracked specimens

Rad. = 1.0
(2.5)

0.5
(1.3)

1.0
(2.5)

6.5
(16.5)

1.5
(3.8)

2.25
(5.7)

(a) Tensile specimen.

0.175
(0.45)

t = 0.04 (0.10)

0.025
(0.063)

(b) Details of surface crack.

Figure 1.- Configuration and details of tensile and precracked specimens. Dimensions are in inches (centimeters).

Loading direction

(a) Specimen strips.

(b) Completed specimen.

(c) Compression-tested, exposed specimen, stress-corrosion damage.

Figure 2.- Bent-beam self-stressed specimen configuration and effect of axial compression on specimens with stress-corrosion damage.

Loading jack

Test liquid container

Microscope and photographic equipment

Test specimen.

Specimen grip

Load cell

Figure 3.- Stress-corrosion test apparatus for surface precracked tensile specimens.

L-68-9923.1

(a) Annealed condition.

(b) Solution-treated condition.

(c) Solution-treated, aged condition.   L-69-5092

Figure 4.- Microstructure of Ti-6Al-4V alloy sheet. Magnification: X 1000.

(a) As-fabricated specimen, σ = 100 ksi (690 MN/m^2).

(b) Solution-treated specimen after 16 hours exposure, σ = 100 ksi (690 MN/m^2).

(c) Annealed specimen compression tested after 500 hours exposure, σ = 50 ksi (345 MN/m^2).

(d) Annealed specimen compression tested after 500 hours exposure, σ = 25 ksi (170 MN/m^2).

Figure 5.- Self-stressed specimens after fabrication and various stages of testing.

L-69-5093

(a) 25 ksi (170 MN/m^2), fractured strip.

(b) 25 ksi (170 MN/m^2), unbroken strip.

(c) 50 ksi (340 MN/m^2), fractured strip.

(d) 50 ski (340 MN/m^2), unbroken strip.

L-69-5094

Figure 6.- Self-stressed specimens compression tested after 500 hours exposure in reagent methanol. Magnification: X 7.25.

Figure 7.- Effect of small chloride ion additions on the environmental cracking of Ti-6Al-4V alloy annealed sheet in reagent methanol. $\sigma = 100$ ksi $(690 \ MN/m^2)$.

Figure 8.- Effect of material condition on the cracking behavior of Ti-6Al-4V alloy in methanol. Self-stressed specimens; $\sigma = 100$ ksi (690 MN/m^2).

Figure 9.- Variation in time to failure with initial applied stress intensity factor K_{Ii} for Ti-6A1-4V alloy sheet in reagent methanol.
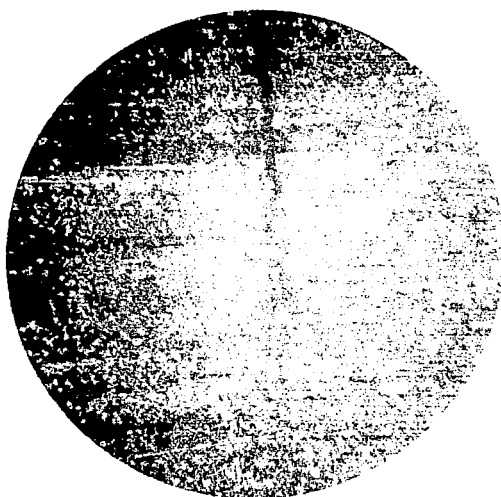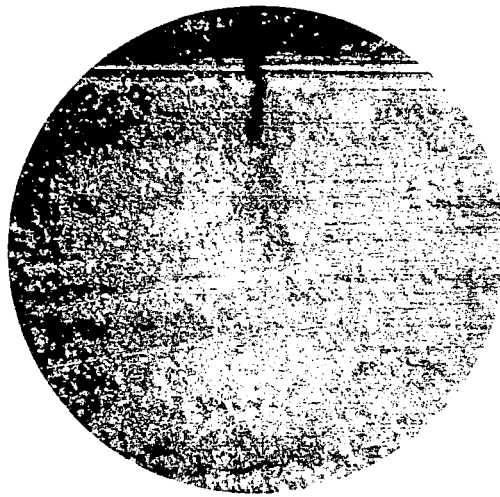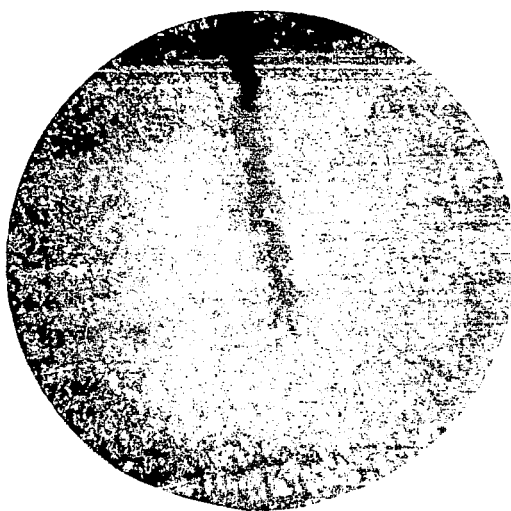
(a) After 13 minutes.

(b) After 28 minutes.

(c) After 44 minutes.

(d) After 1 hour, 17 minutes.

L-69-5095

Figure 10.- Photomicrographs of Ti-6A l-4V annealed sheet crack tip after exposure times indicated in reagent methanol. $K_{1i} = 24.1$ ksi (in.)$^{1/2}$ (26.5 MN/m^2 (m)$^{1/2}$). Magnification: X 100.

34

Fast fracture area

Environmental exposure flaw growth

Initial electrical discharge machining starter notch
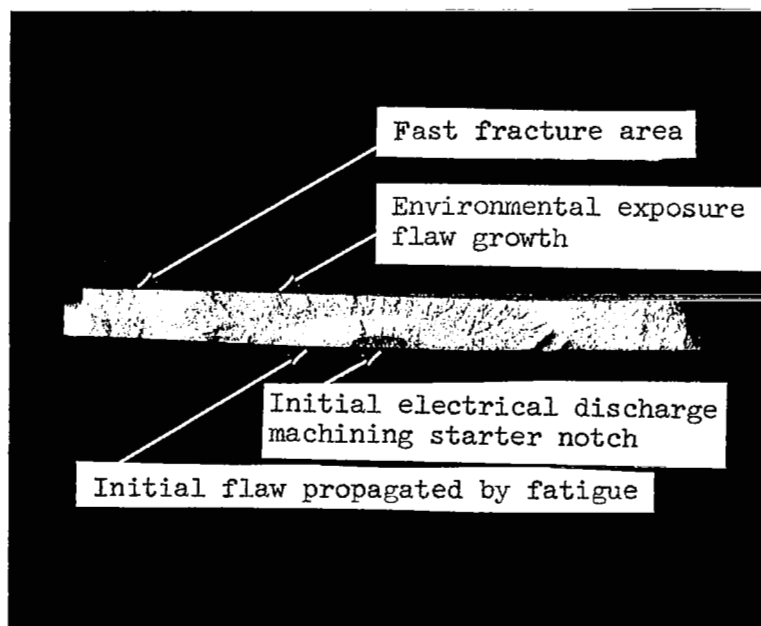
Initial flaw propagated by fatigue

L-69-5096
Figure 11.- Fractograph of Ti-6Al-4V annealed sheet specimen after environmental failure at 1 hour, 20 minutes exposure in reagent methanol. K_{Ii} = 24.1 ksi (in.)$^{1/2}$ (26.5 MN/m^2 (m)$^{1/2}$). Magnification: X 7.

Figure 12.- Variation in time to failure with initial applied stress intensity factor K_{Ii} for Ti-6Al-4V alloy in reagent methanol containing 100 ppm chloride ion.

Figure 13.- Effect of material condition on the cracking behavior of Ti-6Al-4V alloy in methanol. Tensile precracked specimens; $K_{Ii} = 25$ ksi (in.)$^{1/2}$ (27.4 MN/m^2 (m)$^{1/2}$).

(a) After 1 minute.

(b) After 8 minutes.

(c) After 12 minutes.

(d) After 18 minutes.

Figure 14.- Photomicrographs of Ti-6Al-4V sheet, solution-treated, after exposure times indicated in reagent methanol containing 100 ppm chloride ion. $K_{Ii} = 26.6$ ksi $(in.)^{1/2}$ $(29.2$ MN/m^2 $(m)^{1/2})$. Magnification: X 100.

(e) After 23 minutes.

(f) After 28 minutes.

(g) After 38 minutes.

Figure 14.- Concluded.

L-69-5098

Fast fracture area

Environmental exposure
flaw growth

Initial electrical discharge
machining starter notch

Initial flaw propagated by fatigue

Figure 15.- Fractograph of Ti-6Al-4V solution-treated sheet specimen after environmental failure at 40 minutes exposure in reagent methanol containing 100 ppm chloride ion. K_{Ii} = 26.6 ksi (in.)$^{1/2}$ (29.2 MN/m^2 (m)$^{1/2}$). Magnification: X 7.

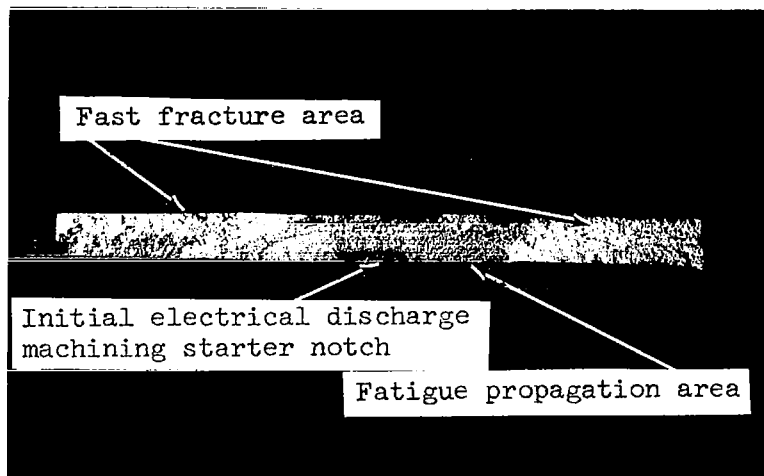Figure 16.- Cross-sectional diagram of deep semielliptical surface crack.

Figure 17.- Apparent K_{Ic} as a function of ratio of crack depth to specimen thickness for Ti-6Al-4V in the annealed condition.

Figure 18.- Fractograph of Ti-6Al-4V alloy sheet in the annealed condition showing details of initial crack and fracture appearance. Magnification: X 7.

Dimensions

Width, 0.5008 in. (1.272 cm)
Thickness, 0.0392 in. (0.100 cm)
Crack length, 0.1984 in. (0.503 cm)
Crack depth, 0.0260 in. (0.066 cm)
Crack depth/thickness, 0.66

Test Results

σ_{ty} = 133.5 ksi (915 MN/m^2)

σ_{g} = 113.0 ksi (780 MN/m^2)

K_{Ic} = 45.5 ksi (in.)$^{1/2}$ (50 MN/m^2 (m)$^{1/2}$)

L-69-5100

"*The aeronautical and space activities of the United States shall be
conducted so as to contribute . . . to the expansion of human knowl-
edge of phenomena in the atmosphere and space. The Administration
shall provide for the widest practicable and appropriate dissemination
of information concerning its activities and the results thereof.*"

—NATIONAL AERONAUTICS AND SPACE ACT OF 1958

NASA SCIENTIFIC AND TECHNICAL PUBLICATIONS

TECHNICAL REPORTS: Scientific and
technical information considered important,
complete, and a lasting contribution to existing
knowledge.

TECHNICAL NOTES: Information less broad
in scope but nevertheless of importance as a
contribution to existing knowledge.

TECHNICAL MEMORANDUMS:
Information receiving limited distribution
because of preliminary data, security classifica-
tion, or other reasons.

CONTRACTOR REPORTS: Scientific and
technical information generated under a NASA
contract or grant and considered an important
contribution to existing knowledge.

TECHNICAL TRANSLATIONS: Information
published in a foreign language considered
to merit NASA distribution in English.

SPECIAL PUBLICATIONS: Information
derived from or of value to NASA activities.
Publications include conference proceedings,
monographs, data compilations, handbooks,
sourcebooks, and special bibliographies.

TECHNOLOGY UTILIZATION
PUBLICATIONS: Information on technology
used by NASA that may be of particular
interest in commercial and other non-aerospace
applications. Publications include Tech Briefs,
Technology Utilization Reports and Notes,
and Technology Surveys.

Details on the availability of these publications may be obtained from:

SCIENTIFIC AND TECHNICAL INFORMATION DIVISION

NATIONAL AERONAUTICS AND SPACE ADMINISTRATION
Washington, D.C. 20546